Calibration and Stochastic Modelling of Inertial Navigation Sensor Errors

Mohammed El-Diasty and Spiros Pagiatakis
Dept. of Earth & Space Science & Engineering, York University, Canada

Abstract

The integration of Global Positioning System (GPS) with an inertial measurement unit (IMU) has been widely used in many applications of positioning and orientation. The performance of a GPS-aided inertial integrated navigation system is mainly characterized by the ability of the IMU to bridge GPS outages. This basically depends on the inertial sensor errors that cause a rapid degradation in the integrated navigation solution during periods of GPS outages. The inertial sensor errors comprise systematic and random components. In general, systematic errors (deterministic) can be estimated by calibration and therefore they can be removed from the raw observations. Random errors can be studied by linear or high order nonlinear stochastic processes. These stochastic models can be utilized by a navigation filter such as, Kalman filter, to provide optimized estimation of navigation parameters. Traditionally, random constant (RC), random walk (RW), Gauss-Markov (GM), and autoregressive (AR) processes have been used to develop the stochastic model in the navigation filters.

In this technical note, the inertial sensor errors are introduced and discussed. Subsequently, a six-position laboratory calibration test is described. Then, mathematical models for RC, RW, GM, and AR stochastic models with associated variances for gyros and accelerometer random errors are presented along with a discussion regarding ongoing research in this field. Also, the implementation of a stochastic model in a loosely coupled INS/GPS navigation filter is explained.

Keywords: GPS, INS, Calibration, Random Error, Stochastic Process.

1. Inertial Sensor Errors

The performance of a GPS-aided inertial navigation system is mainly characterized by the ability of the IMU to bridge GPS outages. This ability of the IMU to bridge GPS outages depends on the inertial sensor errors, which,

if not treated properly, cause a rapid degradation in the integrated navigation solution during the periods of GPS outages. Inertial sensors are used to collect measurements that can be processed using inertial processing software to estimate position, velocity, and attitude that can be integrated with GPS data to provide a complete navigation solution. An inertial sensor is made up of three gyroscopes (shortly gyros), and three accelerometers. A gyro is device that maintains orientation in space, and thus can sense the rate of change of direction (angular rate) of the vehicle on which is mounted. The rate of change of direction (angular rate) can mathematically be integrated to provide attitude changes over time. Similarly, an accelerometer senses linear accelerations, which when integrated in time give velocity changes, and when integrated twice give position changes over time. The major error sources in gyros and accelerometers are biases, and scale errors related to non-orthogonalities of the axes. Hence, due to the integration process, biases and scale errors impose unstable errors in positions, velocities, and attitudes. The growth of these errors depends on the type of inertial sensor used (high, medium and low grade). The inertial sensor errors can be classified into two types, deterministic (systematic) and random (Nassar, 2005).

Major deterministic error sources include bias and scale errors, which can be removed by specific calibration procedures; Park and Gao (2002) discussed such laboratory calibration procedures. However, the inertial sensor random errors primarily include the sensor noise, which consists of two parts, a high frequency and a low frequency component (Skaloud et al., 1999). The high frequency component has white noise characteristics, while the low frequency component is characterized by correlated noise (Skaloud et al., 1999). De-noising methodology is required to filter the high frequency noise in the inertial sensor measurements prior to processing, using a low pass filter, a wavelet or neural network de-noising procedure (El-Rabbany and El-Diasty, 2004). Several studies have focused on evaluating such techniques (Skaloud et al., 1999; Nassar, 2005; Abdel-Hamid et al., 2004). On the other hand, the low frequency

noise component (correlated noise) can be modelled using random processes such as, random constant, random walk, Gauss-Markov or periodic random processes (Nassar, 2005). The most commonly used process is the first-order Gauss-Markov process. The development of the stochastic model for an inertial sensor is one of the most important steps for building a reliable integrated navigation system. The reason is that the inertial sensor propagates large navigation errors in a small time interval. Unless an accurate stochastic model is developed, the mechanization parameters (velocity, attitude, position) will be contaminated by the unmodelled errors and the system performance will be degraded (El-Diasty et al., 2007b).

Let us assume that inertial sensor measurements are denoted by ω_{imu} and f_{imu} representing direction rate of change (angular rate) and linear acceleration, respectively. They can be written approximately as functions of the true direction rate of change ω and the true linear acceleration f in the body frame (because very small inertial sensor second order errors are neglected) as (Titterton, 2004; El-Diasty et al., 2007b):

$$\omega_{imu} \approx [I + S_g + \delta S_g]\omega + b_g + \delta b_g + w_g , \qquad (1)$$

$$f_{imu} \approx [I + S_a + \delta S_a]f + b_a + \delta b_a + w_a , \qquad (2)$$

where:

$$I = \begin{bmatrix} 1 & 0 & 0 \\ 0 & 1 & 0 \\ 0 & 0 & 1 \end{bmatrix}, S_{g,a} = \begin{bmatrix} s_{XX} & s_{XY} & s_{XZ} \\ s_{YX} & s_{YY} & s_{YZ} \\ s_{ZX} & s_{ZY} & s_{ZZ} \end{bmatrix}_{g,a} ,$$

$$\delta S_{g,a} = \begin{bmatrix} \delta s_{XX} & \delta s_{XY} & \delta s_{XZ} \\ \delta s_{YX} & \delta s_{YY} & \delta s_{YZ} \\ \delta s_{ZX} & \delta s_{ZY} & \delta s_{ZZ} \end{bmatrix}_{g,a} , b_{g,a} = \begin{bmatrix} b_X \\ b_Y \\ b_Z \end{bmatrix}$$

$$\delta b_{g,a} = \begin{bmatrix} \delta b_X \\ \delta b_Y \\ \delta b_Z \end{bmatrix}_{g,a} , w_{g,a} = \begin{bmatrix} w_X \\ w_Y \\ w_Z \end{bmatrix}_{g,a}$$

where I is the identity matrix (unitless), S_g and S_a are matrices (unitless) comprising scale errors (diagonal elements) and non-orthogonality errors (non-diagonal elements) of the gyro and accelerometer respectively, b_g and b_a are biases (deg/s for gyros and m/s^2 for accelerometers), δS_g and δS_a are matrices (unitless) comprising residual scale errors (diagonal elements) and residual non-orthogonality errors (non-diagonal elements), δb_g and δb_a are residual biases (deg/s for

gyros and m/s^2 for accelerometers), and w_g and w_a are zero mean white noises (deg/s for gyros and m/s^2 for accelerometers). Biases and scale errors are either estimated through laboratory calibration or can be modelled as additional parameters in Kalman filter. In this study we discuss the laboratory calibration approach that allows the direct estimation of the bias and scale, which we can then remove from the raw measurements ω_{imu} and f_{imu} (i.e. before implementing the inertial mechanization equations). Then, the corrected measurements ω_{ib}^b and f^b (which will be the input to inertial mechanization equations) are:

$$\omega_{ib}^b \approx [I + (\delta S_g)]\omega + (\delta b_g) + w_g , \qquad (3)$$

$$f^b \approx [I + (\delta S_a)]f + (\delta b_a) + w_a . \qquad (4)$$

However, ω_{ib}^b and f^b still contain random errors: δS_g and δS_a are matrices comprising residual scale errors (diagonal elements) and residual non-orthogonality errors of the gyro and accelerometer respectively, δb_g and δb_a are residual biases, and w_g and w_a are zero mean white noises.

The residual biases and residual scale errors are the inertial random errors and can usually be modelled by stochastic models inside a Kalman filter at each epoch and then removed simultaneously from ω_{ib}^b and f^b (epoch by epoch) during the mechanization equation implementation. This stochastic model can be random constant, random walk, or Gauss-Markov process (Grewal et al., 2007; El-Diasty et al., 2007b). The resultant measurements at each epoch are $\hat{\omega}_{ib}^b$ and $\hat{f}^b$, which represent the optimal estimation of the gyro and accelerometer outputs and they can be used to provide an accurate and continuous navigation solution. In the next section we discuss the six-position calibration laboratory test used to estimate the gyro and accelerometer biases and their scale errors (b_g, b_a, S_g, S_a).

2. Laboratory Determinations of Inertial Biases, Scale, and Non-orthogonality Errors

The laboratory calibration of an IMU is well documented in Titterton (2004) and Salychev (1998). Also, Shin and El-Sheimy (2002), and Syed et al. (2007) are two key papers that describe the practical implementation for these calibration methods and show ongoing research in the area of inertial navigation. In laboratory calibration, a six-position static test (up and down position for the three

inertial sensor axes) is commonly performed to collect the gyro and accelerometer measurements. From this test, an estimate of the gyro and accelerometer bias, scale, and non-orthogonality errors can be obtained. The bias is a systematic error called bias offset, which is the offset of the sensor measurement from its true value. The scale error describes the error in the relationship between the sensor output signal and the measured physical quantity. The non-orthogonality error is the error resulting from the imperfection of mounting the inertial sensors along three orthogonal axes at the time of manufacturing. Fig. 1 shows the up and down positions and the excitation (reference) signal in each position (we have a natural excitation signal for accelerometers which is local gravity g in the lab (Salychev, 1998)). We excite the gyro by a known rotational rate ω_{known} using a calibration turntable (Titterton, 2004). Therefore, all three accelerometers can be tested using two-position static tests in the zenith direction, and any gyro sensor can be tested using a two-position dynamic test in any direction (Titterton, 2004). It should be noted that the direction of the known rotational rate ω_{known} in Fig. 1 is the clockwise direction for both, up and down positions.
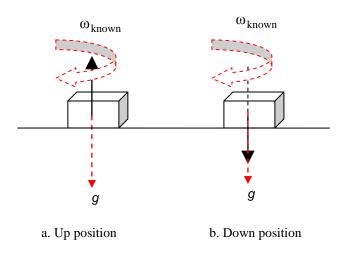

a. Up position   b. Down position

Fig. 1 Up and down positions of the IMU for calibration of one axis – the dotted arrows describe the true excitation (reference) signal.

There are two methodologies that can be employed to find the calibration parameters (b_g, b_a, S_g and S_a). In this technical note, we simply call these two methods six-position direct method and six-position weighted least squares method. In both methods, data are collected in each position for a minimum of 30 seconds (which can give 3000 samples if the sampling rate is 100 Hz). Then the gyro and accelerometer biases (b_g and b_a), scale, and non-orthogonality error matrices (S_g and S_a) can be

calculated. It should be noted that S_g and S_a are matrices comprising the scale errors (diagonal elements) and non-orthogonality errors (non-diagonal elements).

2.1 Six-Position Direct Method

Assume that we want to calibrate the X-axis gyro and accelerometer errors of an IMU. In the direct method the biases and scale errors can only be estimated (but non-orthogonality errors are neglected) from the two positions (X-axis up and X-axis down) by taking the average of the measurements in three steps as follows:

Step1: assume that the gyro and accelerometer measurements at epoch *k* are:

$$\omega_{imu}^{Xup}\Big|_k \approx (1+s_{XXg}+\delta s_{XXg})\cdot(-\omega_{known})+ \\ b_{Xg}+\delta b_{Xg}+w_{Xg} \quad (5)$$

$$f_{imu}^{Xup}\Big|_k \approx (1+s_{XXa}+\delta s_{XXa})\cdot(-g)+ \\ b_{Xa}+\delta b_{Xa}+w_{Xa} \quad (6)$$

$$\omega_{imu}^{Xdn}\Big|_k \approx (1+s_{XXg}+\delta s_{XXg})\cdot(\omega_{known})+ \\ b_{Xg}+\delta b_{Xg}+w_{Xg} \quad (7)$$

$$f_{imu}^{Xdn}\Big|_k \approx (1+s_{XXa}+\delta s_{XXa})\cdot(g)+ \\ b_{Xa}+\delta b_{Xa}+w_{Xa} \quad (8)$$

where Xup means IMU X-axis is in up direction, Xdn means X-axis is in down direction, ω_{known} is known rotational rate and g is the local gravity.

Step2: average the gyro and accelerometer measurements as follows:

$$Av(\omega_{imu}^{Xup}) \approx (1+s_{XXg})\cdot(-\omega_{known})+b_{Xg}, \quad (9)$$

$$Av(f_{imu}^{Xup}) \approx (1+s_{XXa})\cdot(-g)+b_{Xa}, \quad (10)$$

$$Av(\omega_{imu}^{Xdn}) \approx (1+s_{XXg})\cdot(\omega_{known})+b_{Xg}, \quad (11)$$

$$Av(f_{imu}^{Xdn}) \approx (1+s_{XXa})\cdot(g)+b_{Xa}, \quad (12)$$

where Av is the average operator. It should be noted that when the measurements are averaged for one position, noise (w_{Xg} and w_{Xa}) and residual errors ($\delta s_{XXg}, \delta b_{Xg}, \delta s_{XXa}$ and δb_{Xa}) are eliminated because their expected values (mean) are zeros.

Step3: estimate the bias and scale errors using the following equations:

$$b_{Xg} = \frac{Av(\omega_{imu}^{Xdn}) + Av(\omega_{imu}^{Xup})}{2} \, , \qquad (13)$$

$$s_{XXg} = \frac{Av(\omega_{imu}^{Xdn}) - Av(\omega_{imu}^{Xup}) - 2 \cdot \omega_{known}}{2 \cdot \omega_{known}} \, , \qquad (14)$$

$$b_{Xa} = \frac{Av(f_{imu}^{Xdn}) + Av(f_{imu}^{Xup})}{2} \, , \qquad (15)$$

$$s_{XXa} = \frac{Av(f_{imu}^{Xdn}) - Av(f_{imu}^{Xup}) - 2 \cdot g}{2 \cdot g} \, . \qquad (16)$$

The bias and scale errors for Y-axis and Z-axis can be estimated using the same approximate method and steps when Y-axis and Z-axis are configured in the up and down positions, respectively. In this methodology we use two measurements for each axis to estimate the biases and scale errors (in total six measurements are used for the three axes). The advantage of this method lies in its simplicity of implementation. However, the disadvantage is that the non-orthogonality errors can not be estimated.

2.2 Six-Position Weighted Least Squares Method

In this method, all biases, scale errors and non-orthogonality errors for the three axes X, Y and Z are estimated using all the measurements from the six-position configuration. Assume that we wish to estimate the accelerometer errors. From the six-position test we expect to have the following observation equations:

1. when the X-axis is in the up direction, we estimate three averages from the three accelerometers:

$$\begin{bmatrix} Av(f_{imu}^{Xup})_X \\ Av(f_{imu}^{Xup})_Y \\ Av(f_{imu}^{Xup})_Z \end{bmatrix} = \begin{bmatrix} b_X \\ b_Y \\ b_Z \end{bmatrix}_a + \\ \left[\begin{bmatrix} 1 & 0 & 0 \\ 0 & 1 & 0 \\ 0 & 0 & 1 \end{bmatrix} + \begin{bmatrix} s_{XX} & s_{XY} & s_{XZ} \\ s_{YX} & s_{YY} & s_{YZ} \\ s_{ZX} & s_{ZY} & s_{ZZ} \end{bmatrix}_a \right] \cdot \begin{bmatrix} -g \\ 0 \\ 0 \end{bmatrix} \qquad (17)$$

2. when the X-axis is in the down direction we estimate three averages from the three accelerometers:

$$\begin{bmatrix} Av(f_{imu}^{Xdn})_X \\ Av(f_{imu}^{Xdn})_Y \\ Av(f_{imu}^{Xdn})_Z \end{bmatrix} = \begin{bmatrix} b_X \\ b_Y \\ b_Z \end{bmatrix}_a + \\ \left[\begin{bmatrix} 1 & 0 & 0 \\ 0 & 1 & 0 \\ 0 & 0 & 1 \end{bmatrix} + \begin{bmatrix} s_{XX} & s_{XY} & s_{XZ} \\ s_{YX} & s_{YY} & s_{YZ} \\ s_{ZX} & s_{ZY} & s_{ZZ} \end{bmatrix}_a \right] \cdot \begin{bmatrix} g \\ 0 \\ 0 \end{bmatrix} \qquad (18)$$

3. when the Y-axis is in the up direction we estimate three averages from the three accelerometers:

$$\begin{bmatrix} Av(f_{imu}^{Yup})_X \\ Av(f_{imu}^{Yup})_Y \\ Av(f_{imu}^{Yup})_Z \end{bmatrix} = \begin{bmatrix} b_X \\ b_Y \\ b_Z \end{bmatrix}_a + \\ \left[\begin{bmatrix} 1 & 0 & 0 \\ 0 & 1 & 0 \\ 0 & 0 & 1 \end{bmatrix} + \begin{bmatrix} s_{XX} & s_{XY} & s_{XZ} \\ s_{YX} & s_{YY} & s_{YZ} \\ s_{ZX} & s_{ZY} & s_{ZZ} \end{bmatrix}_a \right] \cdot \begin{bmatrix} 0 \\ -g \\ 0 \end{bmatrix} \qquad (19)$$

4. when the Y-axis is in the down direction we estimate three averages from the three accelerometers:

$$\begin{bmatrix} Av(f_{imu}^{Xdn})_X \\ Av(f_{imu}^{Xdn})_Y \\ Av(f_{imu}^{Xdn})_Z \end{bmatrix} = \begin{bmatrix} b_X \\ b_Y \\ b_Z \end{bmatrix}_a + \\ \left[\begin{bmatrix} 1 & 0 & 0 \\ 0 & 1 & 0 \\ 0 & 0 & 1 \end{bmatrix} + \begin{bmatrix} s_{XX} & s_{XY} & s_{XZ} \\ s_{YX} & s_{YY} & s_{YZ} \\ s_{ZX} & s_{ZY} & s_{ZZ} \end{bmatrix}_a \right] \cdot \begin{bmatrix} 0 \\ g \\ 0 \end{bmatrix} \qquad (20)$$

5. when the Z-axis is in the up direction we estimate three averages from the three accelerometers:

$$\begin{bmatrix} Av(f_{imu}^{Zup})_X \\ Av(f_{imu}^{Zup})_Y \\ Av(f_{imu}^{Zup})_Z \end{bmatrix} = \begin{bmatrix} b_X \\ b_Y \\ b_Z \end{bmatrix}_a + \\ \left[\begin{bmatrix} 1 & 0 & 0 \\ 0 & 1 & 0 \\ 0 & 0 & 1 \end{bmatrix} + \begin{bmatrix} s_{XX} & s_{XY} & s_{XZ} \\ s_{YX} & s_{YY} & s_{YZ} \\ s_{ZX} & s_{ZY} & s_{ZZ} \end{bmatrix}_a \right] \cdot \begin{bmatrix} 0 \\ 0 \\ -g \end{bmatrix} \qquad (21)$$

6. when the Z-axis is in the down direction we estimate three averages from the three accelerometers:

$$\begin{bmatrix} Av(f_{imu}^{Zdn})_X \\ Av(f_{imu}^{Zdn})_Y \\ Av(f_{imu}^{Zdn})_Z \end{bmatrix} = \begin{bmatrix} b_X \\ b_Y \\ b_Z \end{bmatrix}_a +$$

$$\left[\begin{bmatrix} 1 & 0 & 0 \\ 0 & 1 & 0 \\ 0 & 0 & 1 \end{bmatrix} + \begin{bmatrix} s_{XX} & s_{XY} & s_{XZ} \\ s_{YX} & s_{YY} & s_{YZ} \\ s_{ZX} & s_{ZY} & s_{ZZ} \end{bmatrix}_a \right] \cdot \begin{bmatrix} 0 \\ 0 \\ g \end{bmatrix}$$

(22)

The collection of the above six observation equations (from Eq. 17 to 22) provides the following single observation equation in matrix form:

$$A \cdot \dot{X} = W \qquad (23)$$

where,

$$A = \begin{bmatrix} -g & g & 0 & 0 & 0 & 0 \\ 0 & 0 & -g & g & 0 & 0 \\ 0 & 0 & 0 & 0 & -g & g \\ 1 & 1 & 1 & 1 & 1 & 1 \end{bmatrix}, \qquad (24)$$

$$W = \begin{bmatrix} Av(f_{imu}^{Xup})_X + g & Av(f_{imu}^{Xdn})_X - g & Av(f_{imu}^{Yup})_X & Av(f_{imu}^{Ydn})_X & Av(f_{imu}^{Zup})_X & Av(f_{imu}^{Zdn})_X \\ Av(f_{imu}^{Xup})_Y & Av(f_{imu}^{Xdn})_Y & Av(f_{imu}^{Yup})_Y + g & Av(f_{imu}^{Ydn})_Y - g & Av(f_{imu}^{Zup})_Y & Av(f_{imu}^{Zdn})_Y \\ Av(f_{imu}^{Xup})_Z & Av(f_{imu}^{Xdn})_Z & Av(f_{imu}^{Yup})_Z & Av(f_{imu}^{Ydn})_Z & Av(f_{imu}^{Zup})_Z + g & Av(f_{imu}^{Zdn})_Z - g \end{bmatrix}$$

…(25)

$$X = \begin{bmatrix} s_{XX} & s_{XY} & s_{XZ} & b_X \\ s_{YX} & s_{YY} & s_{YZ} & b_Y \\ s_{ZX} & s_{ZY} & s_{ZZ} & b_Z \end{bmatrix}_a, \qquad (26)$$

Now we estimate the calibration parameters as follows:

$$\hat{X} = (W \cdot P.A^T) \cdot (A \cdot P.A^T)^{-1}, \qquad (27)$$

where

$$P = \sigma_0^2 \cdot \Sigma^{-1} \qquad (28)$$

is the 6×6 weight matrix, σ_0^2 is the *a-priori* variance factor (usually $\sigma_0^2 = 1$), and Σ is the sample variance-covariance matrix comprising the sample variances of the accelerometer averages from the six-position test in the diagonal and zeros in the non-diagonal elements. The gyro six-position test with least squares estimation follows the same methodology but the 18 average accelerometer measurements $Av(f_{imu}^{\bullet})$ are replaced by the 18 average gyro measurements $Av(\omega_{imu}^{\bullet})$ and the

local gravity g is replaced by the known rotational rate ω_{known} from the turntable.

It should be noted that the static test of high grade inertial sensors can be used to find the scale error of the gyros because the spin of the Earth ($\omega_{Earth} \approx 15.0141 \deg/h$) can be measured. In this case, $\omega_{known} = \omega_{Earth} \cdot \sin(\phi)$ in Eq. (14), where ϕ is the latitude of the inertial sensor position during the calibration test. This case is not valid in the low cost inertial sensors because the Earth's spin is completely buried in high level white noise (low signal to noise ratio). Also, it is worth noting that for low cost inertial sensors, the bias and scale errors are temperature-dependent as indicated by Abdel-Hamid et al. (2004). Therefore, it is strongly recommended to perform the calibration test at different temperature points to estimate the inertial sensor bias and scale errors as functions of temperature.

2.3 Ongoing Research in Calibration

An effective calibration method is the multi-position approach (Shin and El-Sheimy, 2002), based on multiple independent positions of the sensors (18 different positions). This method does not require precise alignment of the IMU axes and can be applied on-the-fly in the field. This method uses the combined three-axis effect of the local gravity and Earth rotational rate to generate the gyro rotational rate excitation signal needed for the calibration. The main disadvantage of this method is that the employed gyro rotation rate excitation signal is the Earth rotational rate, which is a weak signal and can result in observability problems when estimating the scale and non-orthogonality errors. The scale and non-orthogonality errors of low-cost sensors, if not accurately estimated, can contribute significantly to the overall position error during prediction periods (INS-only solutions when GPS outages exist). Thus, instead of using the Earth rotational rate as an excitation signal, Syed et al. (2007) modifies the multi-position calibration method using a rotational rate excitation from a turntable with 26 independent sensor positions (as opposed to the 18 positions in the Earth rotation method). Another advantage of the modified multi-position calibration

method is that the least squares singularity problem is resolved efficiently by providing an accurate initial value for the inertial calibration parameters (for more details see Syed et al. (2007)).

In the next section we discuss the different stochastic processes used to model the three residual biases, scale errors and white noise of the gyros and accelerometers (δb_g δb_a, δS_g, δS_a, w_g and w_a).

3. Stochastic Modelling of Inertial Sensor Errors

Various stochastic processes are well documented in Gelb (1974) and Priestley (1981), and their application in inertial navigation is well documented in Jekeli (2000), Grewal et al. (2007) and Rogers (2003). Also, El-Diasty et al. (2007b), Nassar (2005), Flenniken et al. (2005), and Wall and Bevly (2006) are key papers that describe the practical implementation for these stochastic processes and show ongoing research in the area of inertial navigation. The following terms should be defined first (Gelb, 1974; Priestley, 1981):

- Continuous time signals are signals that are described by an analytical function of time.
- Discrete time signals are signals that have values only at discrete instants of time. Sampling a continuous-time signal generates a discrete signal.
- Stationary stochastic process is a process whose joint probability distribution does not change when shifted in time or space. Consequently, parameters such as the mean and variance, if they exist, also do not change over time or with position.
- Autocorrelation function of a discrete signal is the expected value of the product of a random signal with a time-shifted version of itself. If x(t) is random signal then the autocorrelation equation is $R(\tau) = E(x(t) \cdot x(t + \tau))$, where E is the expectation operator and τ is the time shift. The autocorrelation function is very useful because it tells us the time interval over which a correlation in the noise exists.

As mentioned earlier, four stochastic models are described in this note, namely:

- Random constant model,
- Random walk model,
- Gauss-Markov model,
- Autoregressive model

In addition the Allan variance analysis and ongoing research on stochastic modelling are discussed in this note.

3.1 Random Constant (RC) Model

A random bias can be described as an unpredictable random quantity with a constant value through the following differential equation in continuous time domain (Jekeli, 2000):

$$\dot{x} = 0 . \tag{29}$$

In discrete time, the process is represented by the following equation:

$$x_k = x_{k-1} . \tag{30}$$

The corresponding autocorrelation function $R(\tau)$ is plotted as a function of time shift τ in Fig. 2 (Gelb, 1974):

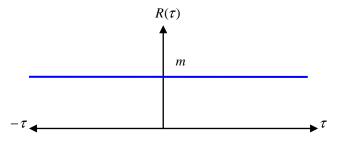Fig. 2 Autocorrelation function of a random constant process.

Therefore, the corresponding variance is:

$$\sigma_{\hat{x}}^2 = m^2 , \tag{31}$$

where m is a constant value. So, the discrete-time random constant model can take the form of Eq. (30) but there is no noise present in this process.

3.2 Random Walk (RW) Model

A Random Walk (RW) process x is a zero-mean Gaussian stochastic process with stationary independent increments i.e., in a RW process the difference $(x_k - x_{k-1})$ is a purely random sequence w_k. A RW can be described through the following differential equation in continuous time domain (Jekeli, 2000):

$$\dot{x} = w . \tag{32}$$

From this equation, it can be seen that RW can be generated by integrating an uncorrelated random sequence w. In discrete time, the process can be described through the following equation (Grewal et al., 2007):

$$x_k = x_{k-1} + w_k . \qquad (33)$$

For a very large number of data samples k, the previous equation converges to:

$$x_k = \sum_{i=1}^{k-1} w_i , \qquad (34)$$

where the mean equals zero and the variance can be derived using the discrete form as follows:

$$\sigma_{x_k}^2 = E\left[x_k^2\right] - \mu_{\hat{x}}^2 = \sum_{i=1}^{k} E\left[w_i^2\right] = k\sigma_w^2 , \qquad (35)$$

$$\sigma_{w_k}^2 = \frac{\sigma_{\hat{x}_k}^2}{k} , \qquad (36)$$

where E is the expectation operator. So, the discrete-time RW model can take the form of Eq. (33) and the variance of the driven noise w_k as Eq. (36). Also, Allan variance analysis can be used to estimate the variance of the driven noise w_k (see section 3.2 for Allan variance details).

3.3 Gauss-Markov Model (Shaping filter)

Gauss-Markov (GM) random processes are stationary processes that have exponential autocorrelation functions. The GM process is important because it is able to represent a large number of physical processes with reasonable accuracy and has a relatively simple mathematical formulation (Gelb, 1974). A stationary Gaussian process that has an exponentially decaying autocorrelation is called first-order GM process. For a random process *x* with zero mean, mean squared error σ^2, and correlation time T_c, the first-order GM model is described by the following continuous-time equation (Gelb, 1974):

$$\dot{x} = -\frac{1}{T_c} x + w \qquad (37)$$

The autocorrelation function (see Fig. 3) of the first-order GM model is given by (Gelb, 1974):

$$R(\tau) = E\left[x(t)x(t+\tau)\right] = \sigma^2 e^{-|\tau|/T_c} \qquad (38)$$

where τ is the time shift, T_c is the correlation time, and σ^2 is the variance at zero time shift ($\tau = 0$). The most important characteristic of the GM process is that it can represent bounded uncertainty which means that any

correlation coefficient at any time shift is less or equal the correlation coefficient at zero time shift $R(\tau) \le R(0)$) (Gelb, 1974).

Two parameters namely, T_c (correlation time) and σ_w^2 (driven noise variance), are required to describe a GM process as shown in Fig. 3.
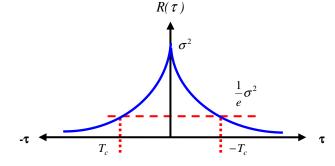

Fig. 3 The autocorrelation function of the first-order Gauss-Markov process.

The first-order GM process in discrete time can be written as (Grewal et al., 2007):

$$x_k = e^{-\Delta t/T_c} x_{k-1} + w_k . \qquad (39)$$

And the associated variance can be given by (Grewal et al., 2007):

$$\sigma_{x_k}^2 = \frac{\sigma_{w_k}^2}{1 - e^{-2\Delta t_k/T_c}} , \qquad (40)$$

$$\sigma_{w_k}^2 = \sigma_{x_k}^2 \left(1 - e^{-2\Delta t_k/T_c}\right). \qquad (41)$$

So, the discrete-time first-order GM model can be applied using Eq. (39) and the variance of the driven noise w_k is given by Eq. (41).

The second-order GM process with zero mean, mean-square error σ^2, and correlation time T_c, is described by the following continuous-time equation (Gelb, 1974):

$$\ddot{X} = -2\beta \cdot \dot{X} - \beta^2 \cdot X + w \qquad (42)$$

where

$$\beta \approx \frac{2.1416}{T_c} . \qquad (43)$$

The autocorrelation function of the second-order GM model is given by (Gelb, 1974):

$$R(\tau) = E[x(t)x(t+\tau)] = \sigma^2 (1 + \beta \cdot |\tau|) \cdot e^{-\beta \cdot |\tau|}$$

$$\ldots (44)$$

An important property of the second-order GM process is that the first derivative of its autocorrelation function equals zero at $\tau = 0$. So, we can solve this equation to find the value of β and then we can estimate the correlation time T_c. For higher order GM-processes see Gelb (1974) for more details.

The first-order GM process is one of the most commonly-applied shaping filters in integrated navigation systems because the bounded uncertainty characteristic of GM process makes it the best model for slowly varying sensor errors such as residual bias and scale errors (Rogers, 2003).

3.4 Autoregressive Model

To avoid the problem of inaccurate modelling of inertial sensor random errors due to inaccurate autocorrelation function determination, we can apply another method for estimating inertial sensor errors as introduced by Nassar (2005). Compared to a first-order GM random process, Autoregressive (AR) processes have more modelling flexibilities since they are not always restricted to only one parameter, and higher orders can be used (Nassar, 2005). In many time series applications, AR processes are used to model (estimate) their stochastic part (Gelb, 1974). The inertial sensor data are considered to form a time series that contain both systematic and stochastic error components, and hence AR models are used to describe the inertial stochastic errors. The GM process given by Eq. (37) is equivalent to an AR process of first-order (Nassar, 2005; El-Diasty et al. 2007b). An AR process is a time series produced by a linear combination of past values and its structure is shown in Fig. 4.
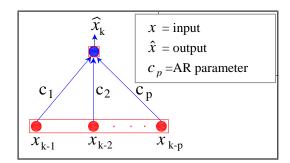

Fig. 4 Autoregressive (AR) structure

An AR process of order p can be described by the following linear equation (Priestley, 1981; El-Diasty et al., 2007a):

$$x_k = \sum_{i=1}^{p} c_i x_{k-i} + w_k, \qquad (45)$$

where x_k is the process output, x_{k-i} are previous system states, and c_i are the AR model parameters. The AR model parameters can be estimated using least-squares fitting (El-Diasty et al., 2007b) or can alternatively be estimated using Yule-Walker, covariance and Burg's methods (Nassar, 2005). The variance of the noise component w_k (is also equivalent to the mean square error MSE in this case because the expected mean of the residual equals zero) can be estimated numerically from the following equation:

$$\sigma^2_{w_k} = \frac{1}{k} \sum_{i=1}^{k} (x_i^d - \hat{x}_i)^2, \qquad (46)$$

where k is the size of the sample of the stationary process, x_k^d is the known value of the process (desired output), and $\hat{x}_k$ is the corresponding estimated output.

If we have a first order AR model, then the discrete form will be (Priestley, 1981):

$$x_k = c_1 \cdot x_{k-1} + w_k \qquad (47)$$

for which the associated variance of the noise component w_k can numerically be estimated from stationary data by Eq. (46) or it can be estimated by using the following equation (Priestley, 1981):

$$\sigma_{w_k} = \begin{cases} \sigma_{x_k} \left(\dfrac{1 - c_1^2}{1 - c_1^{2k}} \right) & \text{if } |c_1| \neq 1 \\ \dfrac{\sigma_{x_k}}{k} & \text{if } |c_1| = 1 \end{cases} \qquad (48)$$

So, the discrete-time first-order AR model can take the form of Eq. (47) and the variance of the driven noise w_k is given by Eq. (46) or Eq. (48). It should be noted that when $c_1 = 1$, the AR process becomes a RW process. The AR model was introduced by Nassar (2005) as an alternative to GM process for the modelling of the residual gyro and accelerometer biases.

3.5 Allan Variance Analysis

Allan variance analysis is commonly and efficiently used to identify and obtain the variances for most of the random errors (IEEE Std. 647-1995, 1998; Hou and El-Sheimy, 2003; El-Diasty et al., 2007a). The Allan variance is a method of representing root mean square random drift error as a function of averaging times. It is simple to compute, much better than having a single RMS drift number to apply to a system error analysis, and relatively simple to interpret and understand. Its most useful application is in the identification and estimation of random drift coefficient in a previously formulated model equation. If N is the number of data points with sampling internal of Δt_0, then a group of n data points (with $n < N/2$ can be created. Each group member is called a cluster T of size $n\Delta t_0$. The Allan variance can be defined in terms of an output variable, calculated at discrete times $x_k = x(kt_0)$. The Allan variance is estimated as follows:

$$\sigma^2(T) = \frac{1}{2T^2(N-2n)} \sum_{k=1}^{N-2n} \left(x_{k+2n} - 2x_{k+n} + x_k\right)^2$$

$$\ldots \ (49)$$

There is a very important relationship between Allan variance and power spectral density (PSD) of a random process:

$$\sigma^2(T) = 4 \int_0^\infty df \cdot S_x(f) \cdot \frac{\sin^4(\pi fT)}{(\pi fT)^2} \qquad (50)$$

where $S_x(f)$ is the power spectral density (PSD) of the random process $x(T)$, namely the instantaneous output rate of the sensor. In the derivation of Eq. (50), it is assumed that the random process $x(T)$ is stationary.

Eq. (50) is the equation that will be used to calculate the Allan variance from the PSD. The different types of random processes can be examined by investigating the Allan variance plot. The Allan variance provides a means of identifying various noise terms that exist in the data. Fig. 5 shows a typical Allan variance curve estimated from gyro measurements. A typical Allan variance curve estimated from accelerometer measurements is the same as from a gyro but the angle random walk and the rate random walk terms should be changed to velocity random walk and the acceleration random walk terms in the plot. There are four possible RW models in inertial navigation systems. The *angle RW* that describes the angular error as a function of time is due to the mathematical integration of the white noise (w_g) of the angular rate (gyro output).

However, the residual bias (b_g) of the gyro can be modelled as rate RW process. On the other hand, the velocity error as a function of time that is due to the mathematical integration of white noise (w_a) of the linear acceleration (accelerometer output) is called velocity RW and the residual bias (b_a) of the accelerometer can be modelled as *acceleration RW* process. The Allan variance terms and algorithm are well documented in IEEE standards (1998)
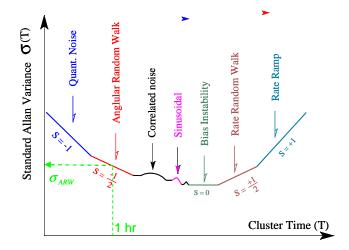

Fig. 5 $\sigma(T)$ Allan variance analysis noise terms results (after IEEE Std. 952-1995, 1998)

It should be noted that different noise terms appear in different regions of T. This property permits easy identification of various random processes that exist in the data. It is well known that the angular and velocity random walk are the dominant noise terms in low cost inertial sensors and therefore we provide in this note how the angle RW (in case of gyros) or velocity RW (in case of accelerometer) can be identified from the Allan plots. The angular random walk process can be identified at T=1h and with a straight line of slope -1/2 as shown in Fig. 5. The noise PSD rate is represented by (IEEE Std. 647-1995, 1998):

$$S_x(f) = \sigma_{ARW}^2, \qquad (51)$$

where σ_{ARW} is the angular random walk coefficient from Fig. 5. Substituting Eq. (51) in Eq. (50) and performing the integration we get:

$$\sigma^2(T) = \frac{\sigma_{ARW}^2}{T}. \qquad (52)$$

The same estimation can be made to find the velocity random walk from process from the typical Allan variance curve of the accelerometer. The identification of the remaining various random processes that exist in the

data can easily be derived using the same methodology given that the slope of Allan variance is well known for any individual random process under investigation as shown in Fig. 5.

3.6 Ongoing Research on Stochastic Modelling

The most commonly used process in stochastic modelling of inertial sensor errors is the first-order Gauss-Markov process, while recently, the use of Autoregressive (AR) modelling methods were tested (Nassar, 2005; Park and Gao, 2002). Nassar (2005) implemented the modelling of the inertial sensor gyro and accelerometer residual biases (three gyros and three accelerometers) using AR processes of different orders and showed that the accuracy of position is improved by almost 50% for second-order AR model and 55% for third-order AR model when compared with the first-order GM and AR model results (Nassar, 2005). However, the number of INS sensor error states is increased from six states to 6×2 for second order AR model or 6×3 for third order AR model. In addition, the implementation of the Kalman filter with large number of states becomes numerically intense and complicates the model excessively (see Nassar, 2005 for more details).

Most recently El-Diasty et al. (2007b) proposed nonlinear stochastic model using wavelet networks. They introduced a new nonlinear stochastic model for inertial sensor residual biases and verified its performance in comparison with first order GM and AR. It was found that the wavelet network-based nonlinear stochastic process can be used to model the highly nonlinear time-varying inertial sensor error. A kinematic test with nine artificial GPS outages of 30s and 60s each showed that the first-order GM and AR stochastic processes give similar results, which agree with the results obtained by Nassar (2005). In addition, the first-order WN-based nonlinear stochastic model gives superior results to the first-order GM and AR processes with an overall improvement of 30% in the 3D position solution for 30s and 60s GPS outages (see El-Diasty et al., 2007b for more details). To this end, in the next section we discuss the implementation of a stochastic model in the INS/GPS navigation filter.

Also, it is worth noting that for low cost inertial sensors, the residual biases are temperature-dependent as indicated by El-Diasty et al. (2007a). Therefore, it is strongly recommended to develop the stochastic model for residual biases at different-temperature points.

4. Stochastic Model Implementation in Loosely-coupled INS/GPS Integration

Methods in which GPS and INS data are integrated differ mostly in the type of data that are shared between the systems. In general however, the following four approaches are the most common (Jekeli, 2000): uncoupled integration, loosely-coupled integration, tight integration, and deep integration. The loosely-coupled and tightly-coupled integration strategies are the most common in practice. In this note we discuss the implementation of the stochastic models in a loosely-coupled integration scheme. In the loosely-coupled integration strategy, position and velocity are used as observations to an INS-only filter. The position and velocity estimates are obtained from a GPS-only filter. This way, the integration approach uses a cascading scheme in which the raw GPS measurements are first processed in a GPS-only filter before they get passed along to aid the INS-only filter (Jekeli, 2000). The inertial navigation error state behaviour is obtained by the perturbation of the INS mechanization equations. This perturbation analysis is well documented in a number of publications, such as Jekeli (2000), Titterton (2004), and Grewal et al. (2007). The error model comprising errors in INS navigation states (i.e., three residual positions δp, three residual velocities δv, and three residual attitudes in Euler angles δA) as well as the INS sensor errors (i.e., three gyro residual biases δb_g, three residual scale errors δs_g, three accelerometer residual biases δb_a, and three residual scale errors δs_a) are used. The system of discrete linearized first-order differential equations for inertial system error model and GPS measurements is used to provide complete navigation solution (positions, velocities and attitude) using INS/GPS integration in standard loosely-coupled mode. The state vector for loosely-coupled INS/GPS error model can be represented by (if we have 21 states):

$$\mathbf{x}_k = \Theta_{k-1} \cdot \mathbf{x}_{k-1} + \mathbf{w}_k, \qquad (53)$$

$$\text{where, } \mathbf{x} = [\delta p_{(1\times3)}, \delta v_{(1\times3)}, \delta A_{(1\times3)}, \big|$$
$$\delta b_{g_{(1\times3)}}, \delta b_{a_{(1\times3)}}, \delta s_{g_{(1\times3)}}, \delta s_{a_{(1\times3)}}]^T,$$

which contains two parts separated by vertical line: The first part is called the inertial dynamic model which contains the three position, velocity and attitude errors ($\delta p_{(1\times3)}, \delta v_{(1\times3)}$ and $\delta A_{(1\times3)}$), which are derived from the perturbation of the INS mechanization equations (see Jekeli, 2000 for this perturbation analysis). The second part is called the stochastic model, which contains the three gyro and accelerometer residual biases and scale errors ($\delta b_{g_{(1\times3)}}, \delta b_{a_{(1\times3)}}, \delta s_{g_{(1\times3)}}$ and $\delta s_{a(1\times3)}$). Θ_{k-1} is the transition matrix which contains the parameters from the dynamic and stochastic model, and

$$\mathbf{w}_k = [w_{\delta v(1\times3)}, w_{\delta A(1\times3)}, w_{bg(1\times3)}, w_{ba(1\times3)}, w_{Sg(1\times3)},$$
$$w_{Sa(1\times3)}]^T$$

is the vector comprising the noise components which follow the standard normal distribution $\mathbf{w}_k \sim N(0, Q_k)$ where Q_k is the covariance matrix with a diagonal form and includes the following variances in a discrete form:

$$Q_k = \text{diagonal}[\sigma^2_{w\delta v(1\times3)}, \sigma^2_{w\delta A(1\times3)}, \sigma^2_{wbg(1\times3)},$$
$$\sigma^2_{wba(1\times3)}, \sigma^2_{wsg(1\times3)}, \sigma^2_{wsa(1\times3)}]^T .$$

The correct identification of the stochastic processes determined above for specific inertial sensors is of major importance in the performance of an integrated model and especially in the ability of a pure inertial solution to bridge data outages. In this note we give an example of how we can extract the stochastic model parameters from the specification sheet of Digital Quartz Inertial (DQI-100) sensor from BEI Systron Donner Inertial Division (BEI, 2004). The DQI is a low cost tactical grade inertial measurement unit based on quartz gyro and accelerometer technology (BEI, 2004).

The first set of parameters to be retrieved comprises the uncertainties ($\sigma_{w\delta v(1\times3)}$ and $\sigma_{w\delta A(1\times3)}$) of the three velocity and attitude error model, respectively. The processes in this case are three angle random walk (ARW) and three velocity random walk (VRW). For simplicity, the ARW and VRW variances are obtained from the specification sheet of DQI-100 (BEI, 2004). Usually, the power densities of ARW and VRW are given in the specification sheet and when we have a dynamic system in the discrete form the associated variances can be estimated as follows:

(1) From DQI-100 specification sheet we know that
$$ARW = 0.035 \, \text{deg}/\sqrt{h} = 2.10 \ \text{deg}/h/\sqrt{Hz} \text{, then for}$$
100 Hz bandwidth (sampling rate of 0.01 sample/sec), the attitude error noise uncertainty equal:
$$\sigma_{w\delta A} = 2.1 \text{deg}/h/\sqrt{Hz} \times \sqrt{100 hz} = 21 \text{deg}/h \ .$$
(2) Again from DQI-100 specification sheet we know that
$$VRW = 60 \, \mu g/\sqrt{Hz} \text{ (where } g \text{ is the local gravity),}$$
then the velocity noise uncertainty equal:
$$\sigma_{w\delta v} = 60 \mu g/\sqrt{Hz} \times \sqrt{100 Hz} = 600 \mu g .$$

Now, we investigate the three gyro and accelerometer residual biases ($\delta b_{g(1\times3)}$ and $\delta b_{a(1\times3)}$). Traditionally, the residual biases are modelled as Gauss-Markov (GM)

processes (Rogers, 2003). The autocorrelation function of the stationary raw data is used to determine the parameters of the Gauss-Markov models. It must be noted however that, prior to the calculation of the autocorrelation function, the inertial sensor data should be de-noised using a low pass filter or wavelet or neural network de-noising. The parameters are derived for each sensor individually. Table 1 shows the correlation time T_b (subscript b means bias) and uncertainty for the residual bias errors from the DQI-100 inertial unit specification sheet (BEI, 2004). Noise uncertainty and correlation time are illustrated in the table.

Table 1 First order GM process parameters

Stochastic model	Correlation Time T_b	Uncertainty σ
Gyros residual bias δb_g	60 s	3 deg/h
Acc residual bias δb_a	60 s	$200 \mu g$

If we consider that the sampling interval is Δt_{k-1} then the GM model for the residual biases can be written as follows:

$$\delta b_k = e^{-\Delta t_{k-1}/60} \delta b_{k-1} + w_{k-1} . \quad (54)$$

We should note that the sampling interval Δt_{k-1} is not exactly constant due to the INS/GPS acquisition and synchronization issues.

Finally, we investigate the three residual scale errors for gyros and accelerometers ($\delta s_{g(1\times3)}$ and $\delta s_{a(1\times3)}$). The scale error is mostly deterministic in nature and only suffers a small residual error due to temperature variation and nonlinearity. It is impossible from the practical point of view, and in static mode, to differentiate the effect of residual scale error and residual bias terms. As such, the residual scale error is modelled as a random constant (RC) (Cannon, 1991). An alternative approach is to model the residual scale error using GM process (Rogers, 2003). In this case, the correlation time T_s (subscript s means scale) and the noise uncertainty will be tuned in the navigation filter to provide the best estimation. It should be noted that the navigation solution in this case will be sub-optimal because the residual scale error parameters used are based on the tuning method and not on a rigorous min/max method.

In summary, if we model the residual bias, and scale errors as GM processes, the stochastic model takes the following form based on the example given in this section:

$$
\begin{bmatrix} \delta b_g^x \\ \delta b_g^y \\ \delta b_g^z \\ \delta b_a^x \\ \delta b_a^y \\ \delta b_a^z \\ \delta s_g^x \\ \delta s_g^y \\ \delta s_g^z \\ \delta s_a^x \\ \delta s_a^y \\ \delta s_a^z \end{bmatrix}_k =
\begin{bmatrix}
c_{bg}^x & 0 & 0 & 0 & 0 & 0 & 0 & 0 & 0 & 0 & 0 & 0 \\
0 & c_{bg}^y & 0 & 0 & 0 & 0 & 0 & 0 & 0 & 0 & 0 & 0 \\
0 & 0 & c_{bg}^z & 0 & 0 & 0 & 0 & 0 & 0 & 0 & 0 & 0 \\
0 & 0 & 0 & c_{ba}^x & 0 & 0 & 0 & 0 & 0 & 0 & 0 & 0 \\
0 & 0 & 0 & 0 & c_{ba}^y & 0 & 0 & 0 & 0 & 0 & 0 & 0 \\
0 & 0 & 0 & 0 & 0 & c_{ba}^z & 0 & 0 & 0 & 0 & 0 & 0 \\
0 & 0 & 0 & 0 & 0 & 0 & c_{sg}^x & 0 & 0 & 0 & 0 & 0 \\
0 & 0 & 0 & 0 & 0 & 0 & 0 & c_{sg}^y & 0 & 0 & 0 & 0 \\
0 & 0 & 0 & 0 & 0 & 0 & 0 & 0 & c_{sg}^z & 0 & 0 & 0 \\
0 & 0 & 0 & 0 & 0 & 0 & 0 & 0 & 0 & c_{sa}^x & 0 & 0 \\
0 & 0 & 0 & 0 & 0 & 0 & 0 & 0 & 0 & 0 & c_{sa}^y & 0 \\
0 & 0 & 0 & 0 & 0 & 0 & 0 & 0 & 0 & 0 & 0 & c_{sa}^z
\end{bmatrix}
\cdot
\begin{bmatrix} \delta b_g^x \\ \delta b_g^y \\ \delta b_g^z \\ \delta b_a^x \\ \delta b_a^y \\ \delta b_a^z \\ \delta s_g^x \\ \delta s_g^y \\ \delta s_g^z \\ \delta s_a^x \\ \delta s_a^y \\ \delta s_a^z \end{bmatrix}_{k-1}
+
\begin{bmatrix} w_{bg}^x \\ w_{bg}^y \\ w_{bg}^z \\ w_{ba}^x \\ w_{ba}^y \\ w_{ba}^z \\ w_{sg}^x \\ w_{sg}^y \\ w_{sg}^z \\ w_{sa}^x \\ w_{sa}^y \\ w_{sa}^z \end{bmatrix}_k
$$

$$\dots (55)$$

where $c_{bg}^x = c_{bg}^y = c_{bg}^z = c_{ba}^x = c_{ba}^y = c_{ba}^z = e^{-\Delta t_{k-1}/60}$, the residual bias error correlation time equals 60s as shown in Table 1 and $c_{sg}^x = c_{sg}^y = c_{sg}^z = c_{sa}^x = c_{sa}^y = c_{sa}^z = e^{-\Delta t_{k-1}/T_s}$ where the residual scale error correlation T_s is tuned (as mentioned before) to the navigation filter to provide the best estimation for positions, velocities and attitudes. The example given here is based on the correlation time being the same for all residual bias errors because we simply used the correlation time from the inertial sensor specification sheet. However, in practice we use static test to collect the three gyro and three accelerometer measurements from the inertial sensors. From the autocorrelation sequence we can estimate three different correlation times for the three gyros residual errors and three different correlation times for the three accelerometers residual biases.

Acknowledgments

References

Abdel-Hamid, W., Osman, A., Noureldin, A. and El-Sheimy, N. (2004) *"Improving the Performance of MEMS-based Inertial Sensors by Removing Short-Term Errors Utilizing Wavelet Multi-Resolution Analysis."* Proceedings of the ION NTM, San Diego, CA.

BEI Technologies, Inc. (2004) *"C-MIGITSTM III User's Guide."* Concord, California 94518-1399, USA.

Cannon, M.E. (1991) *"Airborne GPS/INS with an Application to Aerotriangulation."* Ph.D. thesis, University of Calgary, UCGE Report 20040.

El-Rabbany, A. and El-Diasty, M. (2004) *"An efficient neural network model for de-noising of MEMS-based inertial data."* The Journal of Navigation, 57: 407-415.

El-Diasty, M., A. El-Rabbany, A. and S. Pagiatakis (2007a) *"Temperature Variation Effects on Stochastic Characteristics for Low Cost MEMS-based Inertial Sensor Error."* Measurement Science and Technology, Vol. 18, No.11, pp. 3321-3328.

El-Diasty, M., A. El-Rabbany, A. and S. Pagiatakis (2007b) **"An Accurate Nonlinear Stochastic Model for MEMS-Based Inertial Sensor Error with Wavelet Networks."** Journal of Applied Geodesy Vol. 1, No. 4, pp.201-212.

IEEE Std. 647-1995 (1998) **"IEEE Standard Specification Format Guide and Test Procedure for Single-axis Interferometric Optic Gyros."**

Flenniken, W., Wall, J., Bevly, D.M. (2005) **"Characterization of Various IMU Error Sources and the Effect on Navigation Performance."** Proceedings of ION GNSS, Long Beach, CA.

Gelb, A. (1974) **"Applied Optimal Estimation."** The M.I.T. Press, Cambridge, Massachusetts.

Grewal, M, L. Weill and A. Andrews (2007) **"Global Positioning Systems, Inertial Navigation, and Integration ."** John Wiley & Sons, Inc.

Hou H and El-Sheimy N (2003) **"Inertial sensors errors modeling using Allan variance."** Proceedings of ION GPS, Portland OR.

Jekeli, C. (2000) **"Inertial Navigation Systems with Geodetic Applications."** Walter de Gruyter, New York, NY., USA.

Nassar, S. (2005) **"Accurate INS/DGPS positioning using INS data de-noising and autoregressive (AR) modeling of inertial sensor errors."** Geomatica, 59(3), 283-294.

Park, M. and Gao, Y. (2002) **"Error Analysis of Low-Cost MEMS-based Accelerometers for Land Vehicle Navigation."** Proceedings of ION GPS, Portland, Oregon.

Priestley, M.B. (1981) **"Spectral Analysis and Time Series."** Vol. 1, Academic Press.

Rogers, Robert M. (2003) **"Applied mathematics in integrated navigation systems."** 2nd ed. AIAA education series.

Skaloud, J (1999) **"Optimizing Georeferencing of Airborne Survey Systems by INS/DGPS."** Ph.D. Thesis, Dept. of Geomatics Eng., The University of Calgary, Calgary, Alberta, Canada.

Salychev, O. (1998) **"Inertial Systems in Navigation and Geophysics."** Bauman MSTU Press, Moscow.

Shin, E.-H. and El-Sheimy, N. (2002) **"Accuracy Improvement of Low Cost INS/GPS for Land Applications."** Proceedings of ION NTM, San Diego, CA.

Syed Z. F., Aggarwal P., Goodall C., Niu X. and El-Sheimy N. (2007) **"A new multi-position calibration method for MEMS inertial navigation systems."** Measurements Science and Technology, No. 18 (2007), pp. 1897-1907.

Titterton, D. H. (2004) **"Strapdown inertial navigation technology."** 2nd ed., Radar, sonar, navigations & avionics.

Wall, J. and Bevly, D. M. (2006) **"Characterization of Inertial Sensor Measurements for Navigation Performance Analysis."** Proceedings of the ION GNSS, Fort Worth, TX.